Zitierweise: *Angew. Chem. Int. Ed.* **2025**, *64*, e16389
doi.org/10.1002/anie.202516389

mRNA Therapeutics

Harnessing Deaminated DNA to Modulate mRNA Translation for Controlled and Sequential Protein Expression

*Jihun Choi[+], Tae Ung Jeong[+], Francis Cabanting, Juhyung Song, Cheoljun Park, Seungha Hwang, Jin Young Kang, Jengmin Kang, Linglan Fang, and Yong Woong Jun**

Abstract: Messenger RNA (mRNA) offers transformative potential in vaccines and therapeutics for a range of intractable diseases. While considerable efforts have focused on enhancing protein expression levels to improve efficacy, comparatively little attention has been given to regulating the rate and timing of protein expression. Given that sudden antigen bursts can overstimulate immune responses and pose serious risks in susceptible individuals, precise control over translation kinetics is essential for safe and personalized mRNA therapies. Herein, we describe the use of "damaged" DNA to modulate translation rates of mRNAs. Hybridization of deoxyuridine-containing DNA to the 5′-end of mRNA inhibits translation initiation, which is subsequently displaced via base excision repair (BER), enabling controlled expression. DNA strand lengths determine the rate and onset of translation (e.g., a 52-nt DNA induces a 20-fold slower expression with a 200-min delay). This also enables the sequential expression of multiple mRNAs from a single cocktail. This strategy requires no chemical modification of the mRNA and produces no toxic byproducts, but only recyclable DNA fragments—offering a broadly applicable and biocompatible adjuvant for controlled mRNA translation.

Introduction

Messenger RNA (mRNA) medicines operate by delivering genetic information that directs the synthesis of functional proteins/peptides with pharmacological effects in the human body.[1] Effective mRNA medicines necessitate protein expression levels above the therapeutic threshold, which have been achieved through sequence optimization, mRNA modifications, and advances in mRNA delivery.[2,3] These developments have resulted in a rapid burst of protein expression upon delivery.

Despite their promising efficacy, adverse effects following mRNA drug administration have been noted, which may relate to the human immune system recognizing the expressed proteins as foreign, eliciting a robust immune response.[4] While these adverse effects are generally well tolerated, some individuals experience serious clinical manifestations, including pulmonary embolism, stroke, thrombosis, autoimmunity, and even fatal outcomes.[5–7] Notably, mRNA-based vaccines have been associated with a high prevalence of local side effects, likely due to robust localized protein expression near the inoculation site.[8] Therefore, in future personalized medicine using mRNA, regulating the protein expression rate of mRNA is pivotal for ensuring its safe application. Furthermore, the pharmaceutical industry is increasingly focusing on combination therapies over single-agent treatments, where the sequence and timing of drug administration have a significant impact on therapeutic efficacy.[9] In this context, regulating mRNA translation to achieve sequential protein expression emerges as a promising and essential strategy for future therapies.

Significant efforts have been made to develop chemically modified mRNAs capable of regulating translation through functional groups that can be released upon a trigger (Figure 1a).[10,11] Although introducing multiple chemical modifications to 2′-OH groups or nucleobases offers control over RNA-regulated processes, installing multiple modifications often results in low recovery yield of free mRNA due to residual chemical groups.[12–15] Site-selective modification of mRNA through sequence-specific enzymatic modification has been proposed as a strategy to minimize over-modification, thereby enabling precise control of gene expression.[16,17] A notable advance in this area is the use of synthetic 5′-cap analogues.[11,18,19] As these analogues are essential for translation initiation through recognition by eIF4E, a single modification enables the control of mRNA translation.

While these chemical approaches have successfully demonstrated the control of mRNA translation and opened new research avenues, they are not widely utilized in mRNA pharmaceuticals for clinical trials yet plausibly due to several concerns. First, the activation of mRNA translation releases chemical compounds from the mRNA that are often

[*] J. Choi[+], T. U. Jeong[+], F. Cabanting, J. Song, C. Park, Dr. S. Hwang, Prof. J. Y. Kang, Prof. Y. W. Jun
Department of Chemistry, Korea Advanced Institute of Science and Technology (KAIST), Daejeon 34141, Republic of Korea
E-mail: ywjun@kaist.ac.kr

Dr. J. Kang
Department of Chemistry, Sungkyunkwan University, Suwon 16419, Republic of Korea

Prof. L. Fang
Department of Chemistry, School of Science, Westlake University, Hangzhou 310030, P.R. China

[+] Both authors contributed equally to this work.

Additional supporting information can be found online in the Supporting Information section

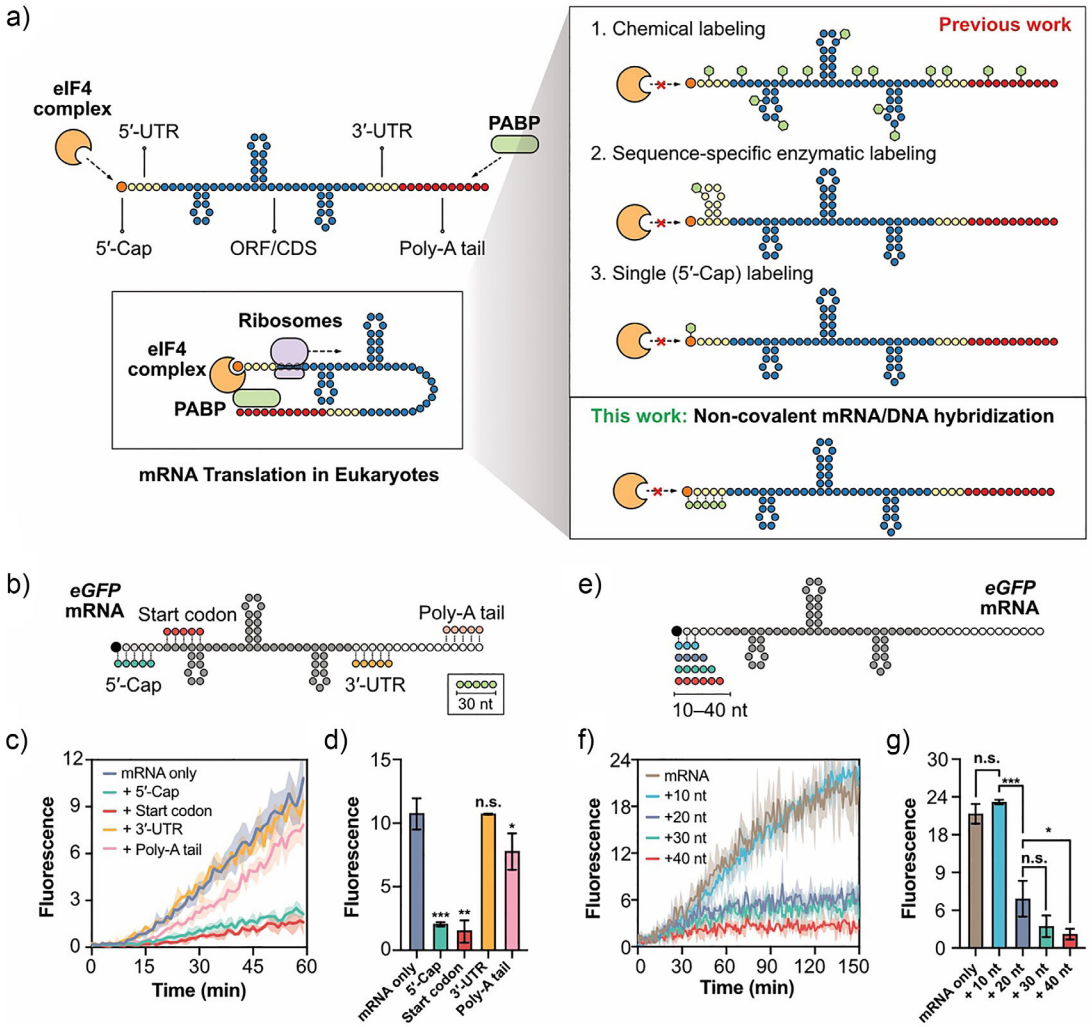

Figure 1. a) Schematic representation of translation initiation involving eukaryotic initiation factors and PABP (left), and different strategies for translation regulation (right). b) Illustration of cDNA hybridizing varied regions on mRNA. c) Real-time fluorescence response of in vitro translation (IVT) of *eGFP* mRNA hybridized with 30-nt cDNA at different regions and d) its fluorescence intensity comparison at 60 min. e) Illustration of different lengths of cDNA hybridized to the 5′-cap region. f) IVT of *eGFP* mRNA hybridized with varying lengths (10–40 nt) of cDNA at the 5′-cap region, and g) its fluorescence intensity comparison at 60 min ($\lambda_{ex} = 485$ nm, $\lambda_{em} = 510$ nm, data represent $n = 3$ independent experiments, $*p < 0.05$, $**p < 0.01$, and $***p < 0.001$).

cytotoxic. Additionally, most triggers required for translation activation are unavailable in the human body. For instance, light activation is hindered by the limited penetration depth of light in tissues, and chemical triggers such as phosphines and hydrogen peroxide are cytotoxic and challenging to control in vivo.[20] Moreover, the complexity of synthesizing and purifying these chemically modified mRNA negates the primary advantage of mRNA medicine, which is its easy programmability. An ideal biochemical method to regulate the translation rates of mRNA should meet the following criteria: i) ease of preparation, ii) absence of toxic chemical release upon activation, and iii) availability of an efficient and ubiquitous trigger within the human body.

Herein, we report the use of deaminated/damaged DNA (dDNA) as an mRNA adjuvant to regulate translation rates. Hybridization of the complementary DNA (cDNA) longer than 20-nt at the 5′-UTR significantly inhibits mRNA translation through interference with the translation initiation process. The use of dDNA, where several thymidine (dT) residues are replaced with deoxyuridine (dU) that provides nearly identical base pairs, maintains this inhibition while allowing full recovery of mRNA translation via base excision repair (BER) by uracil-DNA glycosylase (UDG). We demonstrate that transfecting mRNA hybridized with varied lengths of dDNA enables controlled protein expression in cells, which is further utilized for the sequential protein expression of an mRNA cocktail.

Results and Discussion

Regulation of mRNA Translation in Vitro via Hybridization with Deaminated DNA

mRNA translation is initiated by the binding of eukaryotic translation initiation factors (eIFs) and poly(A) binding

protein (PABP) to the 5′-UTR and poly(A) tail, respectively, forming a "closed-loop" structure that recruits ribosomes (Figure 1a).[21] Previous chemical strategies have involved caging of these regions to disrupt their interactions with translation initiation factors, followed by gradual release of the caging groups to modulate the kinetic profile of protein expression. We hypothesized that hybridizing cDNA to these mRNA sites critical for translation initiation would similarly prevent the binding of initiation factors.

We synthesized 30-nt deoxyoligonucleotides (ODNs) complementary to the 5′-cap region, the start codon region, the 3′-UTR, and the poly(A) tail of *eGFP* mRNA (Figure 1b and Table S1). The mRNA hybridized with each cDNA was subjected to in vitro translation (IVT) using wheat germ extract, monitoring fluorescence enhancement at 510 nm (λ_{ex} = 485 nm) to assess eGFP expression (Figure 1c,d). Hybridizing cDNA to the 5′-cap and start codon regions significantly inhibited translation initiation, plausibly due to interference with translation initiation factors or ribosomes. In contrast, hybridizing cDNA to the 3′-UTR showed nearly identical translation efficiency to that of free mRNA. Surprisingly, even the addition of an excess amount of 30-nt poly-dT to mRNA with a 120-nt poly(A) tail only reduced translation efficiency by 20%–30%, despite poly(A) tail's pivotal role in translation initiation (Figure S2). This may be due to the incomplete coverage of the poly(A) tail by the shorter cDNA, even at high concentrations, owing to the lack of sequence specificity. More likely, the relatively lower binding affinity of rA-dT base pairs and subsequent displacement by PABP may contribute to these observations. Given that cDNA annealing appears to affect translation, we assessed the effects of cDNA length (10–40 nt) on translation inhibition (Figure 1e). The results show that cDNAs longer than 20-nt significantly inhibited mRNA translation, while 10-nt cDNA had little effect, which is consistent with Tm calculations (Figures 1f,g and S3). Longer cDNA exhibited stronger inhibition due to higher binding affinity to mRNA, which can be harnessed in regulating the translation rate in cells (see below).

Next, we explored methods to re-initiate mRNA translation. We anticipated that base excision repair (BER), which begins with the excision of a damaged base, could be utilized to displace the cDNA by reducing its binding affinity with mRNA. Additionally, as BER is highly conserved process in cells, the use of damaged DNA could provide the ubiquitous regulation of mRNA release. dU, a common deaminated DNA base excised by glycosylases such as UDG and SMUG1, was selected as the damaged base for two reasons.[22] First, the binding affinity of dU to adenine is almost identical to that of dT, as dU and dT share a similar structural motif (Figure 2a). This suggests that a simple replacement of dT with dU in DNA can provide comparable translation inhibition through hybridization while allowing displacement from mRNA through the excision by glycosylases. More importantly, the glycosylase must recognize lesions within DNA/RNA hybrids, which adopt an A-form helix. While most glycosylases have evolved to recognize lesions in B-form dsDNA, UDG can exceptionally recognize and excise dU from DNA/RNA hybrids.[23]

The 30-nt DNA strands containing either seven dT or seven dU residues, complementary to the 5′-cap and start codon regions, were subjected to the IVT inhibition assay (Figure 2b and Table S1). mRNA hybridized with the strand containing dU residues (dDNA) exhibited the same level of translation inhibition as those containing dT, confirming a similar binding mode. Translation recovery was then tested upon the treatment of UDG on mRNA hybridized with dDNA (Figure 2c). Treatment with 2.5 units of UDG fully restored mRNA translation when the dDNA was hybridized at the 5′-cap region, whereas recovery was only ~50% when dDNA was hybridized at the start codon (Figure 2d,e). The extent of translation recovery correlated with UDG activity, indicating that glycosylase-mediated disruption of the mRNA–DNA interaction is critical for re-initiating mRNA translation (Figures 2f and S4). In the same manner, reducing the number of deaminated bases in the DNA strands decreased the recovery efficiency of mRNA translation (Figure 2g).

Regulation of Translation Rates in Cells Using Varied Lengths of dDNA

Based on the successful regulation of mRNA translation in vitro, we next sought to test the regulation of mRNA translation in cells. One concern in leveraging endogenous DNA repair activity to re-initiate mRNA translation is that most DNA repair enzymes are primarily localized in the nucleus, where the genomic DNA is stored. In contrast, mRNA is transported to and translated into proteins in the cytosol. However, as DNA repair enzymes are synthesized in the cytosol before nuclear import, we envisioned that sufficient glycosylase activity might be present even in the cytosol to initiate mRNA translation. First, subcellular localization images of UDG and SMUG1 in U2OS cells, obtained from the Human Protein Atlas, indicate the presence of dU-repairing glycosylases in the cytosol (Figure S5).[24] To assess glycosylase activity in the cytosol, cytosolic fractions extracted from U2OS cells were incubated with dU-containing ODNs (Figure 3a). The cleavage pattern of the ODNs was consistent with that observed for dU-ODNs treated with UDG and aniline, which accelerates strand cleavage at AP sites via β-elimination under acidic conditions (Figure 3b). Addition of 2 U UGI (uracil-DNA glycosylase inhibitor) to the lysate markedly reduced the cleavage, supporting AP site formation. These results suggest the presence of UDG and APE1 activities in the cytosol. To further confirm AP site formation, we employed an AP-site-specific fluorescence probe.[25,26] Incubation of dU-ODNs with cytosolic extracts from six different cell lines produced a significant fluorescence enhancement, whereas the addition of 2 U UGI to U2OS lysate completely abolished the fluorescence enhancement, further supporting AP site formation (Figure 3c).

The *eGFP* mRNAs hybridized with either intact or deaminated 60-nt DNA in the 5′-cap region were transfected into U2OS cells that showed the highest cytosolic glycosylase activity in vitro. The mRNA hybridized with the dDNA showed much brighter green fluorescence from eGFP

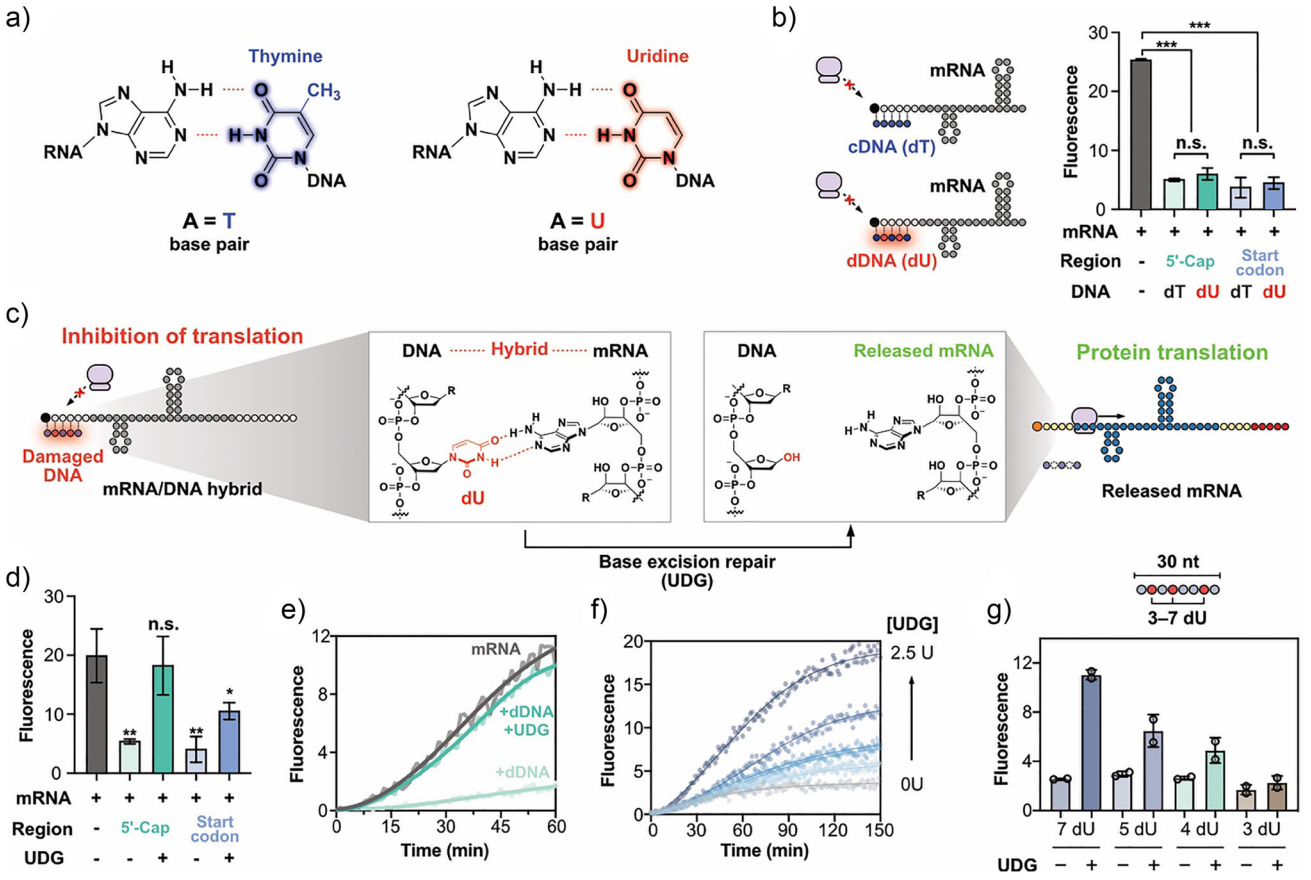

Figure 2. a) Chemical structures of thymine–adenine and uridine–adenine base pairs. b) IVT inhibition assay using complementary strands containing either dT or dU. c) Depiction of translation inhibition by deaminated DNA and re-initiation upon repair by UDG, along with the chemical structures of DNA/RNA hybrid before and after repair. d) Comparison of fluorescence intensity from the 60-min translation of *eGFP* mRNA hybridized with the 30-nt dDNA at the 5′-cap and start codon regions in the presence or absence of 2.5 U UDG. e) Real-time fluorescence enhancement during IVT of *eGFP* mRNA and mRNA hybridized with dDNA at the 5′-cap region in the presence or absence of 2.5 U UDG. f) Kinetic comparison of IVT of *eGFP* mRNA hybridized with dDNA at the 5′-cap region upon treatment with varying concentrations of UDG (0–2.5 U). g) Fluorescence intensity comparison after IVT of *eGFP* mRNA hybridized with 30-nt dDNA containing varying numbers of dU (3–7) at the 5′-cap region for 60 min.

expression under confocal microscopy than that of the one with intact DNA (Figure 3d). The results were consistent with flow cytometric analysis in A549, U2OS, and HEK293T cells, which exhibit significant DNA repair activities in their cytosolic fraction (Figure S6). Time-dependent flow cytometric analysis of the *eGFP* mRNA hybridized with the deaminated one showed gradual protein expression for over 48 h in U2OS cells (Figure 3e). When the same *eGFP* mRNA/DNA hybrids were transfected into NIH/3T3 cells, which exhibited little dU-excision activity in vitro, the protein expression level was negligible, indicating the importance of DNA repair activity in the cytosol for initiating the translation of mRNA/DNA hybrid (Figure 3f).

As the protein expression rate of the mRNA/DNA hybrid depends on the time required for DNA strand displacement by glycosylase activity, we anticipated that dDNA of varied lengths (22–60 nt) containing 5–11 dU residues would enable the regulation of protein expression. Cells transfected with these mRNA/DNA hybrids exhibited different fluorescence intensities after 24 h of incubation, reflecting variations in protein expression rates (Figure 3g,h). In addition, a lower number of dU residues in the 52-nt DNA resulted in reduced protein expression, which is consistent with in vitro data (Figure 3i). The translation rate of the mRNA/DNA hybrid was further investigated through live-cell imaging and western blot analysis (Figures 3j and S7). These results demonstrate that hybridizing mRNA with dDNAs of varied lengths enables the regulation of translation rates and allows for a more than 10-fold reduction in the rate (Figure 3k). Furthermore, hybridization with dDNAs showed delayed translation, suggesting interference with the translation initiation. While mRNA alone showed a burst of protein expression within 30 min after transfection, mRNA/DNA hybrids showed a significant delay in translation, over 3 h when hybridized with the 52-nt strand. Considering that mRNA transfection via lipofectamine takes around 30 min, these results confirm the instant and robust protein expression of naked mRNA in cells, which explains the localized protein expression near the inoculation site of mRNA vaccines. Consequently, the ability of mRNA/DNA hybrid to delay protein expression is expected to facilitate the systemic circulation of mRNA before translation occurs.

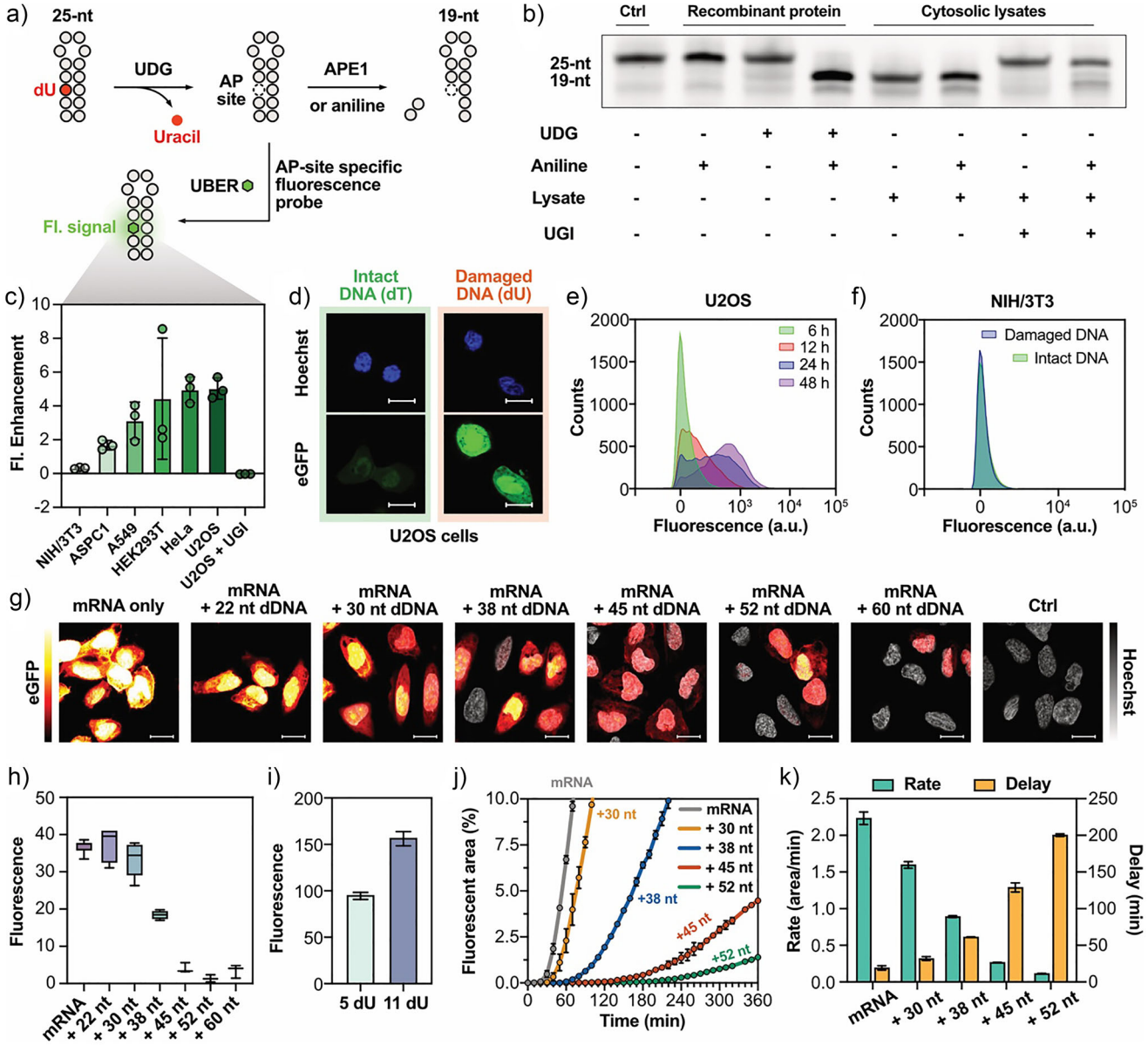

Figure 3. a) Schematic illustration of the experimental setup for detecting glycosylase activity in the cytosol using dU-containing ODNs. b) PAGE analysis of dU-containing ODNs, showing glycosylase and endonuclease activity in cytosolic lysates. c) Quantification of AP site generation demonstrating glycosylase activity in the cytosolic fraction of varied cell lines in the absence or presence of 2 U UGI. d) Confocal microscopic images of U2OS cells transfected with mRNA hybridized with either intact or deaminated DNA. e) Flow cytometric analysis data of *eGFP* mRNA hybridized with 60-nt dDNA translation over time in U2OS cells. f) Flow cytometry comparison of mRNA translation in samples hybridized with either intact or deaminated DNA acquired 24 h post-transfection. g) Fluorescence microscopic images of U2OS cells transfected with mRNA hybridized with dDNA of varied lengths (22–60 nt) and stained with Hoechst (3 μg μL^{-1}). Confocal images were acquired in 24 h post-transfection (λ_{ex} = 488 nm, λ_{em} = 500–550 nm). Scale bar = 20 μm. h) and i) Fluorescence intensity comparison of cells transfected with mRNA hybridized with 60-nt dDNAs of (h) varied lengths or (i) a varied number of uridine. j) Fluorescence enhancement upon *eGFP* mRNA translation with varying dDNA lengths, measured in U2OS cells using the live-cell instrument (IncuCyte). k) Comparison of translation rate and delay extracted from Figure 3j.

Sequential Protein Expression from a mRNA Cocktail Using Deaminated DNA

The delay of protein expression by dDNA was further applied to achieve sequential protein expression from an mRNA cocktail (Figure 4a). When a cocktail of *eGFP* and *mCherry* mRNAs was transfected into U2OS cells, both proteins were expressed simultaneously, exhibiting comparable fluorescence signals (Figure 4b). To control the sequence of protein expression, a 38-nt dDNA targeting *mCherry* mRNA was added to the mRNA cocktail before the transfection into U2OS cells. Within 2–4 h post-transfection, eGFP fluorescence emerged first, while mCherry expression remained negligible under microscopy (Figure 4c and S8). After 6 h, mCherry fluorescence became detectable, confirming the sequential protein expression from the mRNA cocktail. Alternatively,

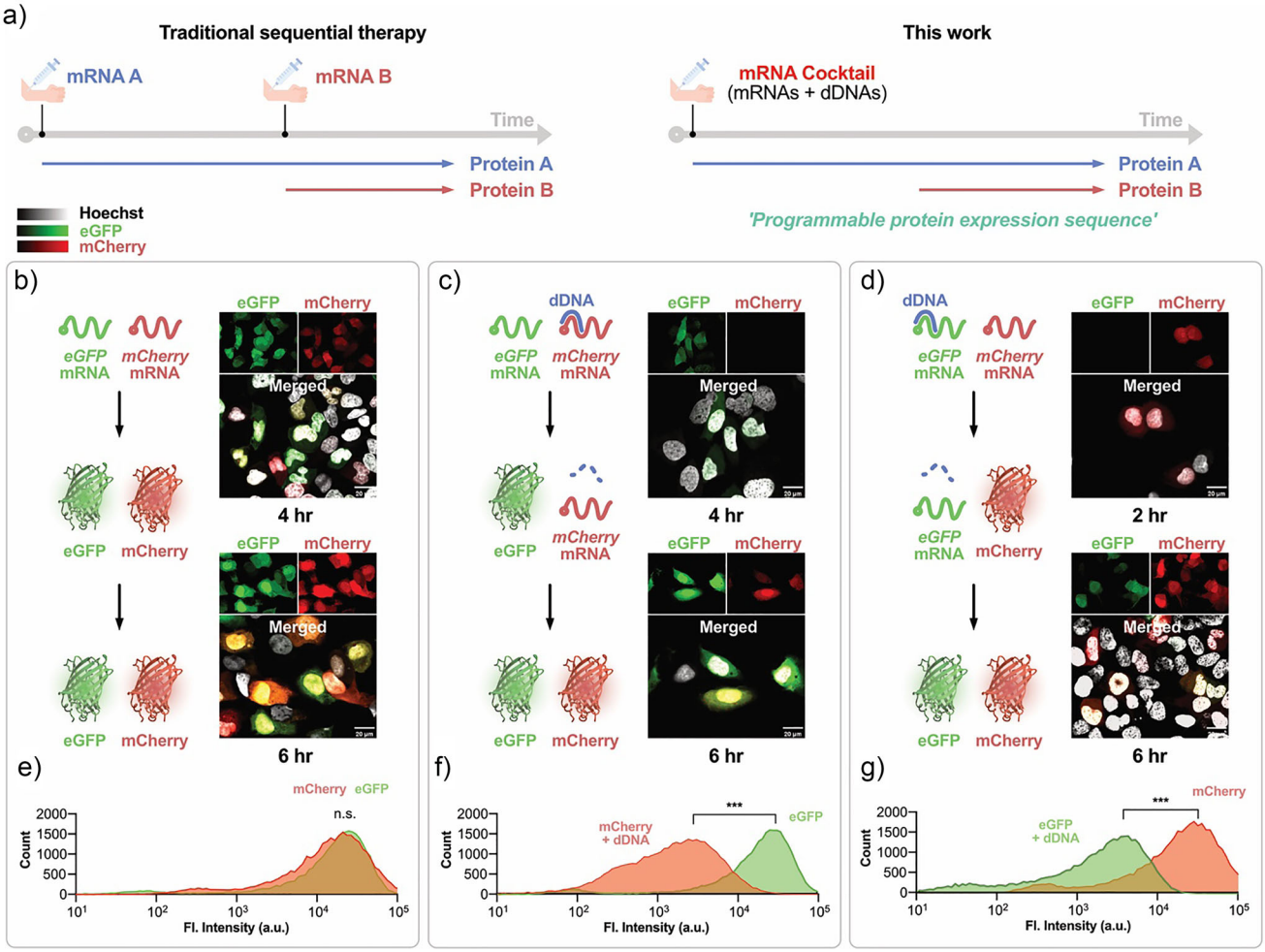

Figure 4. a) Schematic representation of sequential mRNA therapy by traditional multiple injections and mRNA/DNA cocktails. Confocal images of U2OS cells stained with 3 μg μL^{-1} of Hoechst after the transfection with *eGFP* and *mCherry* mRNAs hybridized with b) no dDNA, c) the 38-nt deaminated DNA for *mCherry* mRNA, or d) the 38-nt deaminated DNA for *eGFP* mRNA. e)–g) Flow cytometric analysis of *eGFP* and *mCherry* mRNA translation hybridized with dDNA. The data was acquired in 4 h post-transfection ($N = 3$). Images were taken at 2, 4, and 6 h post-transfection (λ_{ex} = 488 nm and λ_{em} = 500–550 nm for eGFP) and (λ_{ex} = 561 nm and λ_{em} = 570–616 nm for mCherry).

mCherry protein expression preceded eGFP expression when dDNA targeting *eGFP* mRNA was added to the mRNA cocktail (Figure 4d). Flow cytometric analysis also indicates the sequential protein expression (Figure 4e–g).

Cellular Compatibility of mRNA/dDNA Hybrid Therapeutics

We evaluated three key cellular constraints relevant to the therapeutic use of mRNA/dDNA hybrids: RNase H activity, innate immune response, and mRNA stability. First, we investigated the effect of RNase H in cellular experiments. Interestingly, mRNA hybridized with dDNA in the 3′-UTR—where cDNA showed minimal inhibitory effect in vitro—resulted in negligible protein expression in cells, suggesting mRNA degradation by RNase-H activity, along with a possible protective effect in the 5′-cap region against RNase H (Figure 5a). We envisioned that the crowded environment in the 5′-cap region, occupied by initiation factors or ribosomes, sterically hinders the interaction with RNase H. To test the crowding effect in the 5′-cap region in vitro, mRNA hybridized with dDNA at either the 5′-cap region or 3′-UTR was treated with RNase H in the presence or absence of wheat germ extract containing all the components required for in vitro translation. RT-qPCR quantification of the remaining mRNA revealed that the presence of wheat-germ extract led to a ~30-fold increase in stability at the 5′-cap region against RNase H, while having little effect on the 3′-UTR (Figure S9). These results demonstrate a protective role of translation-related components at the 5′-cap region against RNase H-mediated degradation.

Next, to assess the innate immune response of mRNA/dDNA hybrids, we first monitored early-phase signaling using genetically modified THP-1 dual reporter cells that allow the detection of NF-κB activity via secreted embryonic alkaline phosphatase (SEAP). Hybridization of 30-nt or 60-nt DNA (deaminated or intact) to the 5′-cap region of mRNA produced little NF-κB activation compared with mRNA alone (Figure 5b). To further examine late-phase transcriptional feedback, we measured expression levels of

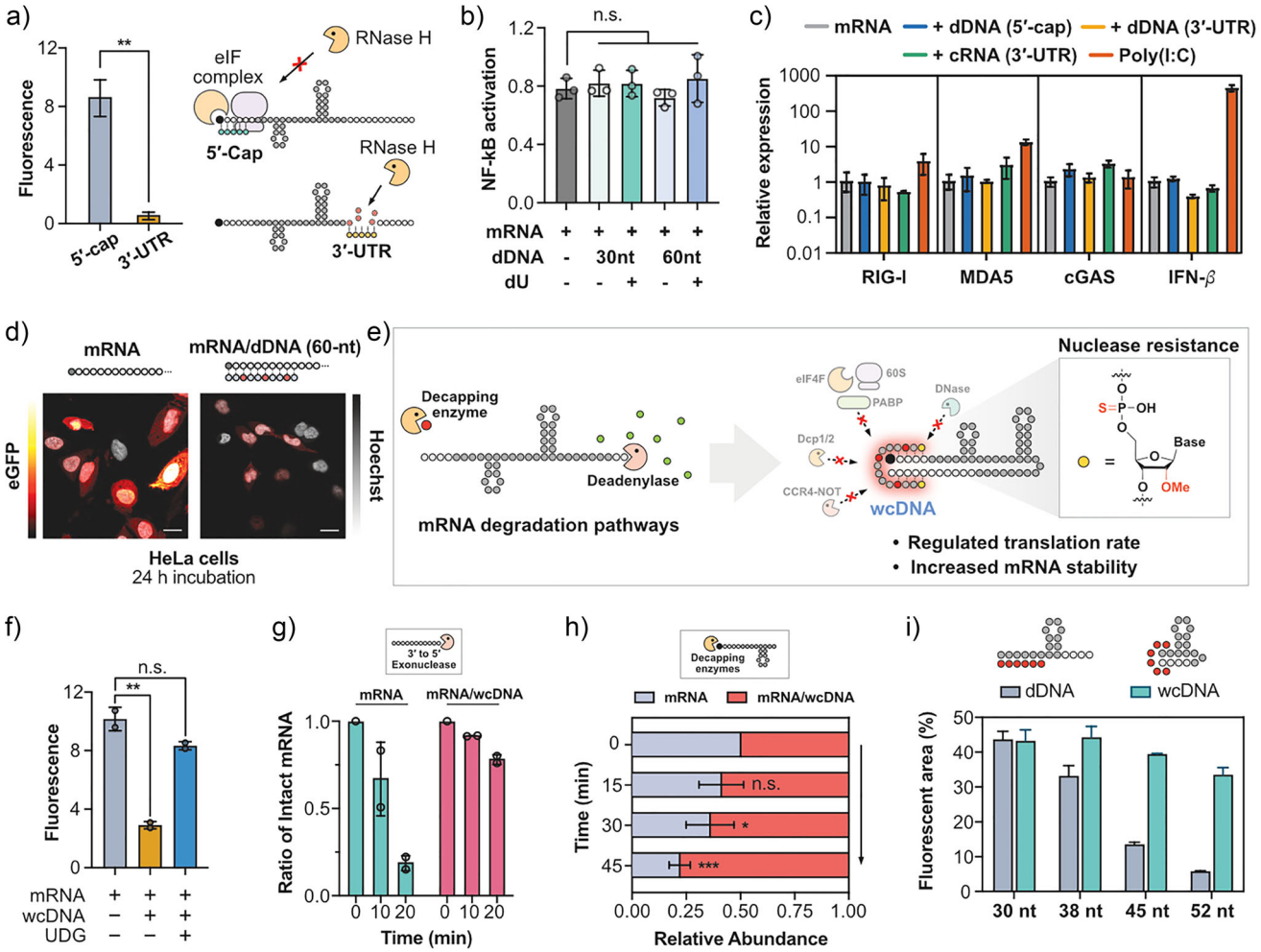

Figure 5. a) Fluorescence intensity comparison of HeLa cells transfected with *eGFP* mRNA hybridized with dDNA at either the 5′-cap region or 3′-UTR, measured after 24 h of incubation ($N = 3$). b) Comparison of NF-κB activation in THP-1 cells transfected with mRNA or mRNA/dDNA hybrid using SEAP activity of THP-1 dual cells 24 h after treatment. c) RT-qPCR analysis of *RIG-I*, *MDA5*, *cGAS*, and *IFN-β* in THP-1 cells transfected with mRNA, mRNA/dDNA, mRNA/cRNA, or poly(I:C) 24 h after treatment. The mRNA levels of each gene were normalized to TBP (or RPLP0) ($N = 3$). d) Fluorescence microscopic images of HeLa cells transfected with *eGFP* mRNA hybridized with 60-nt dDNA and incubated for 24 h. Scale bar = 50 μm. e) Depiction of the wrapping cDNA (wcDNA) design that attenuates enzymatic mRNA degradation, along with the chemical structures of cDNA modifications. f) IVT of *eGFP* mRNA hybridized with wcDNA in the presence or absence of UDG. g) and h) Agarose gel electrophoresis analysis of mRNA degradation by (g) 1 U of Exonuclease T and (h) 0.2 U of mDCP1 and 0.1 U of XRN1 at 37 °C. i) Fluorescent area in U2OS cells transfected with mRNA hybridized with either cDNA or wcDNA of varied lengths (30–52 nt), measured 12 h post-transfection.

key cytosolic sensors such as RIG-I, MDA5, and cGAS, and the downstream mediator IFN-β 24 h after treatment. These genes represent central nodes in cytosolic dsRNA and dsDNA sensing pathways, providing a sensitive read-out for delayed innate immune activation. Consistent with the early reporter assay, no significant changes in expression were detected at this later stage (Figure 5c). In contrast, the positive control poly(I:C) elicited a robust transcriptional response, confirming the responsiveness of the system. These results indicate that, under the tested parameters of DNA length, binding site, and concentration, mRNA/dDNA hybrids trigger negligible innate immune activation both at the early response and the later phase. Nevertheless, as DNA/RNA hybrids have been reported to engage the cGAS pathway, a more comprehensive evaluation will be necessary to fully exclude potential immune responses in therapeutic settings, particularly at higher doses for clinical trials and in combination with lipid nanoparticle delivery systems.

Lastly, while hours of delay in protein expression is expected to exhibit several advantageous features, the innate instability of mRNA, which leads to short half-life, inevitably compromises the overall level of protein expression.[27] For instance, the use of 60-nt dDNAs in HeLa cells exhibited significantly lower fluorescence intensity compared to that from mRNA alone (Figure 5d). In this context, utilizing mRNA stabilization chemistry, such as 2′-OH acylation, in combination with this technique is expected to have a synergistic effect.[13] Alternatively, minor adjustments in dDNA design can effectively mitigate mRNA degradation.

The major enzymatic degradation processes of mRNAs in cells are mediated by two enzymes: deadenylases shortening poly(A) tails and decapping enzymes removing the 5′-cap

(Figure 5e). To mitigate these processes, the binding site of dDNA was adjusted to interfere not only with translation but also with the interactions involving the degradative proteins. The dDNA is designed to wrap around mRNA via hybridization with both the 5′-cap region and the poly(A) tail, thereby preventing both translation and the enzymatic degradation pathways (Figure 5e). This design is enabled by the intrinsic spatial proximity between the 5′- and 3′-termini of mRNA.[28] Additionally, to increase the resistance of the DNA strand against enzymatic degradation, two nucleotides at both ends are modified with 2′-OMe and phosphorothioate groups. It was confirmed that such wrapping cDNA design (wcDNA) is indeed hybridized with both the 5′-cap region and the poly(A) tail, and introducing the modified nucleotides two nucleotides away from dU barely affects repair activity (Figures 5f, S11, and S12).

In vitro enzymatic degradation process from the 3′-end was assessed using exonuclease T (exoT), which has 3′–5′ nuclease activity (Figures 5g and S13). We found that incubation of *eGFP* mRNA with one unit of exoT digested ~80% mRNA in 20 min at 37 °C. In contrast, mRNA hybridized with 52-nt wcDNA showed significantly mitigated degradation, digesting only around 25%. The decapping efficiency was also assessed by using mDCP along with XRN1, which degrades mRNA only in the absence of the 5′ cap from 5′- to 3′-end. When 0.2 unit of mDCP and 0.1 unit of XRN1 are treated for 45 min at 37 °C, mRNA/wcDNA hybrid exhibited much higher stability against the decapping enzyme compared to the nonhybridized mRNA (Figures 5h and S14). Consistently, wcDNAs also enhanced protein expression levels compared to the original dDNA in cells (Figure 5i). Interestingly, the stabilization effects of the wcDNA were more pronounced with longer DNA strands. The results reflect the protective roles during the translation delay; 30-nt wcDNA, which exhibited negligible delay, showed nearly identical protein expression levels to the original dDNA design, whereas longer strands, which caused a substantial delay, resulted in significantly higher protein expression levels. These findings demonstrate that the wrapping design of dDNA enhances mRNA stability against enzymatic degradation, effectively modulating translation rates.

Conclusion

Precise regulation of mRNA translation is recognized as a critical factor in mRNA therapeutics, and considerable efforts have been made to achieve this through chemical modifications of mRNA. In this study, we introduce a simple yet effective strategy to control mRNA translation using deaminated DNA (dDNA), in which dT residues are substituted with deoxyuridine. This approach eliminates the need for direct modifications of mRNA, which is often costly and labor-intensive. Formation of an mRNA/dDNA hybrid at the 5′-cap region effectively suppresses translation by interfering with initiation factor binding while being resistant to RNase H-mediated degradation, presumably due to the crowded environment created by recruited initiation factors. Upon the glycosylase activity of UDG, the first enzyme in the BER pathway, the uracil bases are excised from the DNA, releasing functional mRNA and enabling controlled protein expression.

Transfection of mRNA/dDNA into cells demonstrated precise temporal control of mRNA translation, achieved by tuning the length of dDNA and leveraging the endogenous BER pathway. The ability to modulate translation in cells offers several advantages for the safe administration of mRNA therapeutics. First, since rapid and localized translation of mRNA drugs can induce unintended immune responses and adverse side effects, mRNA/dDNA hybrids can mitigate these concerns by regulating the translation rates and enabling systemic circulation before translation initiates. Additionally, this strategy offers the programmable sequence of protein expression from an mRNA cocktail, optimizing the efficacy of combination mRNA therapies where the order of protein expression is critical for personalized therapeutic success.

While controlled translation offers several key advantages, the innate instability of mRNA in cells compromises total protein expression. Therefore, integrating mRNA-stabilizing strategies, such as 2′-OH acylation, alongside this technique is expected to be synergistic. As an alternative, we have described an mRNA termini-protecting wrapping cDNA design, in which the dDNA binds both the 5′-UTR and poly(A) tail, effectively shielding mRNA from exonucleases, the key mediators of mRNA degradation.

Importantly, this approach relies on a straightforward annealing procedure with dDNA, preserving the ease of programmability and scalability of mRNA therapeutics. This not only avoids the challenges associated with modified mRNA production, which can be expensive and technically demanding, but also maintains exceptional biocompatibility. The DNA strands used in this approach introduce minimal cytotoxicity and can even be recycled in vivo, making them ideal candidates for broader clinical applications in precision medicine.

Supporting Information

The authors have cited additional references within the Supporting Information.[29–35]

Author Contributions

Jihun Choi and Tae Ung Jeong performed the majority of the experiments. Francis Cabanting measured in vitro translation of mRNA. Juhyung Song performed the cell-based experiments related to RNase H activity. Cheoljun Park measured immune responses in cells. Seungha Hwang conducted gel electrophoresis. Jengmin Kang led the immune response experiments. Jin Young Kang and Linglan Fang assisted in project supervision and manuscript preparation. Yong Woong Jun conceived and led the project and wrote the manuscript.

Acknowledgements

This work was supported by the National Research Foundation of Korea (NRF) grant funded by the Korean Government (MSIT) (RS-2024-00346077). The authors thank Prof. Haeshin Lee for kindly providing several cell lines, Prof. Won Do Heo for the U2OS, A549, AsPC-1, and NIH/3T3 cell lines, and Prof. Suk-Jo Kang for the THP-1 dual cell line.

Conflict of Interests

The authors declare no conflict of interest.

Data Availability Statement

The data that support the findings of this study are available from the corresponding author upon reasonable request.

Keywords: Base excision repair · DNA repair · mRNA therapeutics · Regulated mRNA translation · Sequential expression

[1] C. Liu, Q. Shi, X. Huang, S. Koo, N. Kong, W. Tao, *Nat. Rev. Cancer* **2023**, *23*, 526–543, https://doi.org/10.1038/s41568-023-00586-2.
[2] E. Rohner, R. Yang, K. S. Foo, A. Goedel, K. R. Chien, *Nat. Biotechnol.* **2022**, *40*, 1586–1600, https://doi.org/10.1038/s41587-022-01491-z.
[3] B. R. Anderson, H. Muramatsu, S. R. Nallagatla, P. C. Bevilacqua, L. H. Sansing, D. Weissman, K. Karikó, *Nucleic Acids Res.* **2010**, *38*, 5884–5892, https://doi.org/10.1093/nar/gkq347.
[4] I. P. Trougakos, E. Terpos, H. Alexopoulos, M. Politou, D. Paraskevis, A. Scorilas, E. Kastritis, E. Andreakos, M. A. Dimopoulos, *Trends Mol. Med.* **2022**, *28*, 542–554, https://doi.org/10.1016/j.molmed.2022.04.007.
[5] N. Barda, N. Dagan, Y. Ben-Shlomo, E. Kepten, J. Waxman, R. Ohana, M. A. Hernán, M. Lipsitch, I. Kohane, D. Netzer, B. Y. Reis, R. D. Balicer, *N. Engl. J. Med.* **2021**, *385*, 1078–1090, https://doi.org/10.1056/NEJMoa2110475.
[6] N. P. Klein, N. Lewis, K. Goddard, B. Fireman, O. Zerbo, K. E. Hanson, J. G. Donahue, E. O. Kharbanda, A. Naleway, J. C. Nelson, S. Xu, W. K. Yih, J. M. Glanz, J. T. B. Williams, S. J. Hambidge, B. J. Lewin, T. T. Shimabukuro, F. DeStefano, E. S. Weintraub, *J. Am. Med. Assoc.* **2021**, *326*, 1390, https://doi.org/10.1001/jama.2021.15072.
[7] M. Patone, L. Handunnetthi, D. Saatci, J. Pan, S. V. Katikireddi, S. Razvi, D. Hunt, X. W. Mei, S. Dixon, F. Zaccardi, K. Khunti, P. Watkinson, C. A. C. Coupland, J. Doidge, D. A. Harrison, R. Ravanan, A. Sheikh, C. Robertson, J. Hippisley-Cox, *Nat. Med.* **2021**, *27*, 2144–2153, https://doi.org/10.1038/s41591-021-01556-7.
[8] M. Klugar, A. Riad, M. Mekhemar, J. Conrad, M. Buchbender, H. P. Howaldt, S. Attia, *Biology* **2021**, *10*, 752, https://doi.org/10.3390/biology10080752.
[9] B. Yang, H. Liang, J. Xu, Y. Liu, S. Ma, Y. Li, C. Wang, *Int. J. Pharm.* **2025**, *670*, 125156, https://doi.org/10.1016/j.ijpharm.2024.125156.
[10] L. Chen, Y. Liu, W. Guo, Z. Liu, *Exploration* **2022**, *2*, 20210099, https://doi.org/10.1002/EXP.20210099.
[11] N. Klöcker, F. P. Weissenboeck, M. van Dülmen, P. Špaček, S. Hüwel, A. Rentmeister, *Nat. Chem.* **2022**, *14*, 905–913.
[12] W. A. Velema, E. T. Kool, *Nat. Rev. Chem.* **2020**, *4*, 22–37, https://doi.org/10.1038/s41570-019-0147-6.
[13] L. Fang, L. Xiao, Y. W. Jun, Y. Onishi, E. T. Kool, *Nat. Chem.* **2023**, *15*, 1296–1305, https://doi.org/10.1038/s41557-023-01246-6.
[14] F. P. Weissenboeck, H. Schepers, A. Rentmeister, *Angew. Chem. Int. Ed.* **2023**, *62*, e202301778.
[15] S. Qin, X. Tang, Y. Chen, K. Chen, N. Fan, W. Xiao, Q. Zheng, G. Li, Y. Teng, M. Wu, X. Song, *Signal Transduct. Target. Ther.* **2022**, *7*, 166, https://doi.org/10.1038/s41392-022-01007-w.
[16] D. Zhang, C. Y. Zhou, K. N. Busby, S. C. Alexander, N. K. Devaraj, *Angew. Chem. Int. Ed.* **2018**, *57*, 2822–2826, https://doi.org/10.1002/ange.201710917.
[17] D. Zhang, S. Jin, X. Piao, N. K. Devaraj, *ACS Chem. Biol.* **2020**, *15*, 1773–1779, https://doi.org/10.1021/acschembio.0c00205.
[18] S. Ogasawara, *ACS Chem. Biol.* **2017**, *12*, 351–356.
[19] A. Bollu, N. Klöcker, P. Špaček, F. P. Weissenboeck, S. Hüwel, A. Rentmeister, *Angew. Chem. Int. Ed.* **2023**, *62*, e202209975, https://doi.org/10.1002/ange.202209975.
[20] R. Shioi, E. T. Kool, *Chem. Sci.* **2024**, *15*, 15968–15982, https://doi.org/10.1039/D4SC05317F.
[21] J. Brito Querido, I. Díaz-López, V. Ramakrishnan, *Nat. Rev. Mol. Cell Biol.* **2024**, *25*, 168–186, https://doi.org/10.1038/s41580-023-00624-9.
[22] H. E. Krokan, F. Drabløs, G. Slupphaug, *Oncogene* **2002**, *21*, 8935–8948, https://doi.org/10.1038/sj.onc.1205996.
[23] Y. W. Jun, E. M. Harcourt, L. Xiao, D. L. Wilson, E. T. Kool, *Nat. Commun.* **2022**, *13*, 5043, https://doi.org/10.1038/s41467-022-32494-8.
[24] P. J. Thul, L. Åkesson, M. Wiking, D. Mahdessian, A. Geladaki, H. Ait Blal, T. Alm, A. Asplund, L. Björk, L. M. Breckels, A. Bäckström, F. Danielsson, L. Fagerberg, J. Fall, L. Gatto, C. Gnann, S. Hober, M. Hjelmare, F. Johansson, S. Lee, C. Lindskog, J. Mulder, C. M. Mulvey, P. Nilsson, P. Oksvold, J. Rockberg, R. Schutten, J. M. Schwenk, Å. Sivertsson, E. Sjöstedt, et al., *Science* **2017**, *356*, eaal3321.
[25] D. L. Wilson, E. T. Kool, *J. Am. Chem. Soc.* **2019**, *141*, 19379–19388, https://doi.org/10.1021/jacs.9b09812.
[26] Y. W. Jun, E. Albarran, D. L. Wilson, J. Ding, E. T. Kool, *Angew. Chem. Int. Ed.* **2022**, *61*, e202111829, https://doi.org/10.1002/ange.202111829.
[27] C. Wang, H. Liu, *Sci. Rep.* **2022**, *12*, 7259, https://doi.org/10.1038/s41598-022-11339-w.
[28] W. C. Lai, M. Kayedkhordeh, E. V. Cornell, E. Farah, S. Bellaousov, R. Rietmeijer, E. Salsi, D. H. Mathews, D. N. Ermolenko, *Nat. Commun.* **2018**, *9*, 4328, https://doi.org/10.1038/s41467-018-06792-z.
[29] J. SantaLucia Jr., D. Hicks, *Annu. Rev. Biophys.* **2004**, *33*, 415–440, https://doi.org/10.1146/annurev.biophys.32.110601.141800.
[30] N. R. Markham, M. Zuker, *Methods Mol. Biol.* **2008**, *453*, 3–31.
[31] N. E. Watkins Jr., J. SantaLucia Jr., *Nucleic Acids Res.* **2005**, *33*, 6258–6267, https://doi.org/10.1093/nar/gki918.
[32] J. Santa Lucia Jr., *Methods Mol. Biol.* **2007**, *402*, 3–34.
[33] S. Torgasin, K. H. Zimmermann, *Int. J. Bioinf. Res. Appl.* **2010**, *6*, 82, https://doi.org/10.1504/IJBRA.2010.031294.
[34] R. Owczarzy, A. V. Tataurov, Y. Wu, J. A. Manthey, K. A. McQuisten, H. G. Almabrazi, K. F. Pedersen, Y. Lin, J. Garretson, N. O. McEntaggart, C. A. Sailor, R. B. Dawson, A. S. Peek, *Nucleic Acids Res.* **2008**, *36*, W163–W169, https://doi.org/10.1093/nar/gkn198.
[35] A. Untergasser, I. Cutcutache, T. Koressaar, J. Ye, B. C. Faircloth, M. Remm, S. G. Rozen, *Nucleic Acids Res.* **2012**, *40*, e115, https://doi.org/10.1093/nar/gks596.

Manuscript received: July 26, 2025
Revised manuscript received: October 15, 2025
Manuscript accepted: October 17, 2025
Version of record online: November 06, 2025